REPORT DOCUMENTATION PAGE

Form Approved
OMB No. 0704-0188

1. REPORT DATE *(DD-MM-YYYY)*	2. REPORT TYPE	3. DATES COVERED *(From - To)*
30-Sep-2009	REPRINT	

4. TITLE AND SUBTITLE
PROGRESS TOWARDS NEXT GENERATION,WAVEFORM BASED THREE-DIMENSIONAL MODELS AND METRICSTO IMPROVE NUCLEAR EXPLOSION MONITORING IN THE MIDDLE EAST

5a. CONTRACT NUMBER
FA8718-08-C-0009

5b. GRANT NUMBER

5c. PROGRAM ELEMENT NUMBER
62601F

6. AUTHOR(S)
Brian Savage[1], Daniel Peter[2], Brian M. Covellone[1], Arthur J. Rodgers[3], and Jeroen Tromp[2]

5d. PROJECT NUMBER
1010

5e. TASK NUMBER
SM

5f. WORK UNIT NUMBER
A1

7. PERFORMING ORGANIZATION NAME(S) AND ADDRESS(ES)
University of Rhode Island
70 Lower College Rd.
Kingston, RI 02881-1967

8. PERFORMING ORGANIZATION REPORT NUMBER

9. SPONSORING / MONITORING AGENCY NAME(S) AND ADDRESS(ES)
Air Force Research Laboratory
29 Randolph Road
Hanscom AFB, MA 01731-3010

10. SPONSOR/MONITOR'S ACRONYM(S)
AFRL/RVBYE

11. SPONSOR/MONITOR'S REPORT NUMBER(S)
AFRL-RV-HA-TR-2009-1075

12. DISTRIBUTION / AVAILABILITY STATEMENT
Approved for Public Release; Distribution Unlimited.

University of Rhode Island[1], Princeton University[2], and Lawrence Livermore National Laboratory[3]

13. SUPPLEMENTARY NOTES
Reprinted from: Proceedings of the 2009 Monitoring Research Review – Ground-Based Nuclear Explosion Monitoring Technologies, 21 – 23 September 2009, Tucson, AZ, Volume I pp 194 - 200.

14. ABSTRACT

Efforts to update current wave speed models of the Middle East require a thoroughly tested database of sources and recordings. Recordings of seismic waves traversing the region from Tibet to the Red Sea will be the principal metric in guiding improvements to the current wave speed model. Precise characterizations of the earthquakes, specifically depths and faulting mechanisms, are essential to avoid mapping source errors into the refined wave speed model. Errors associated with the source are manifested in amplitude and phase changes. Source depths and paths near nodal planes are particularly error prone as small changes may severely affect the resulting wavefield. Once sources are quantified, regions requiring refinement will be highlighted using adjoint tomography methods based on spectral element simulations (Komatitsch and Tromp, 1999).

An initial database of 250 regional Middle Eastern events from 1990–2007, was inverted for depth and focal mechanism using teleseismic arrivals (Kikuchi and Kanamori, 1982) and regional surface and body waves (Zhao and Helmberger, 1994). From this initial database, we reinterpreted a large, well-recorded subset of 201 events through a direct comparison between data and synthetics based upon a centroid moment tensor inversion (Liu et al., 2004). Evaluation was done using both a 1D reference model (Dziewonski and Anderson, 1981) at periods greater than 80 seconds and a 3D model (Kustowski et al., 2008) at periods of 25 seconds and longer. The final source reinterpretations will be within the 3D model, as this is the initial starting point for the adjoint tomography. Transitioning from a 1D to 3D wave speed model shows dramatic improvements when comparisons are done at shorter periods, e.g., 25 s. Synthetics from the 1D model were created through mode summations while those from the 3D simulations were created using the spectral element method.

Finally, efforts continue in developing the infrastructure required to "quickly" generate event kernels at the nth iteration and invert for a new, $(n+1)$th, wave speed model of the Middle East. While development of the infrastructure proceeds, initial tests using a limited number of events demonstrate that the 3D model, while showing vast improvement compared to the 1D model, still requires substantial modifications. Employing our new, full source set and iterating the adjoint inversions at successively shorter periods will lead to significant changes and refined wave speed structures of the Middle East.

15. SUBJECT TERMS
Seismic velocity models, Moment tensors, Synthetic seismograms, Middle East

16. SECURITY CLASSIFICATION OF:			17. LIMITATION OF ABSTRACT	18. NUMBER OF PAGES	19a. NAME OF RESPONSIBLE PERSON
a. REPORT	b. ABSTRACT	c. THIS PAGE			Robert J. Raistrick
UNCLAS	UNCLAS	UNCLAS	SAR	7	19b. TELEPHONE NUMBER *(include area code)*

PROGRESS TOWARDS NEXT GENERATION, WAVEFORM BASED THREE-DIMENSIONAL MODELS AND METRICS TO IMPROVE NUCLEAR EXPLOSION MONITORING IN THE MIDDLE EAST

Brian Savage[1], Daniel Peter[2], Brian M. Covellone[1], Arthur J. Rodgers[3], and Jeroen Tromp[2]

University of Rhode Island[1], Princeton University[2], and Lawrenee Livermore National Laboratory[3]

Sponsored by the Air Force Research Laboratory and the National Nuelear Security Administration

Contraet No. FA8718-08-C-0009
Proposal No. BAA08-79

ABSTRACT

Efforts to update eurrent wave speed models of the Middle East require a thoroughly tested database of sourees and reeordings. Reeordings of seismie waves traversing the region from Tibet to the Red Sea will be the prineipal metrie in guiding improvements to the current wave speed model. Preeise eharaeterizations of the earthquakes, speeifieally depths and faulting meehanisms, are essential to avoid mapping souree errors into the refined wave speed model. Errors associated with the source are manifested in amplitude and phase ehanges. Souree depths and paths near nodal planes are partieularly error prone as small changes may severely affect the resulting wavefield. Onee sourees are quantified, regions requiring refinement will be highlighted using adjoint tomography methods based on speetral element simulations (Komatitsch and Tromp, 1999).

An initial database of 250 regional Middle Eastern events from 1990–2007, was inverted for depth and focal mechanism using teleseismie arrivals (Kikuehi and Kanamori, 1982) and regional surfaee and body waves (Zhao and Helmberger, 1994). From this initial database, we reinterpreted a large, well-reeorded subset of 201 events through a direet eomparison between data and syntheties based upon a eentroid moment tensor inversion (Liu et al., 2004). Evaluation was done using both a 1D referenec model (Dziewonski and Anderson, 1981) at periods greater than 80 seeonds and a 3D model (Kustowski et al., 2008) at periods of 25 seeonds and longer. The final souree reinterpretations will be within the 3D model, as this is the initial starting point for the adjoint tomography. Transitioning from a 1D to 3D wave speed model shows dramatic improvements when eomparisons are done at shorter periods, e.g., 25 s. Syntheties from the 1D model were ereated through mode summations while those from the 3D simulations were created using the spectral element method.

To further assess errors in source depth and focal mechanism, comparisons between the three methods were made. These comparisons help to identify problematic stations and sources whieh may bias the final solution. Estimates of standard errors were generated for each event's source depth and focal mechanism to identify poorly eonstrained events. A final, well-characterized set of sourees and stations will be used to iteratively improve the wave speed model of the Middle East. After a few iterations during the adjoint inversion proeess, the sourees will be reexamined and reloeated to further reduee mapping of source errors into struetural features.

Finally, efforts eontinue in developing the infrastrueture required to "quickly" generate event kernels at the n^{th} iteration and invert for a new, $(n+1)^{th}$, wave speed model of the Middle East. While development of the infrastrueture proeeeds, initial tests using a limited number of events demonstrate that the 3D model, while showing vast improvement compared to the 1D model, still requires substantial modifications. Employing our new, full source set and iterating the adjoint inversions at sueeessively shorter periods will lead to signifieant ehanges and refined wave speed struetures of the Middle East.

OBJECTIVES

Improved models of 3D wave speeds within the greater Middle East, from the Turkish Plateau to the eastern edge of Tibet (Figure 1), will increase our ability to discriminate between natural and man-made events, locate these events, identify source depths, and determine magnitudes. Current wave speed models of the Middle East will be improved through an adjoint tomography method to iteratively update the models in three dimensions. The initial step towards any well-constrained tomography model involves the compilation of a database of relocated and characterized set of sources and waveforms. Events have been re-inverted in 1D and 3D and agree fairly well with currently available solutions. The adjoint tomography method (Tromp et al., 2005) uses full seismic waveforms as a measure of misfit of the current model iteration. Using the differences between data and synthetics, adjoint sources are constructed and used to generate kernels required to update the current iteration model. In future years, an improved wave speed model of the Middle East will be presented and distributed, built on the foundation of the seismic waveform data set.

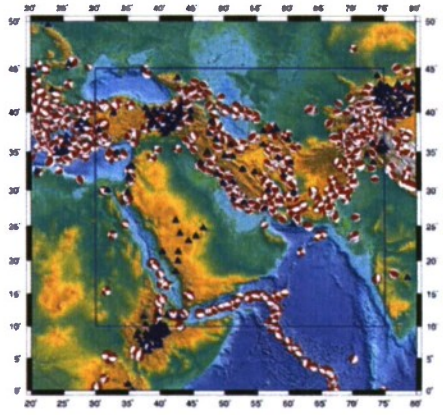

Figure 1. Map of the available sources and stations in the Middle East for the adjoint tomographic inversion.

RESEARCH ACCOMPLISHED

Tomographic updates will use starting model S2.9EA (Kustowski et al., 2008), but to avoid mapping source errors into the wave speed model, sources need to be re-evaluated within this model. Re-evaluation includes an assessment of the faulting parameters and locations using full waveforms. Multiple evaluations were conducted using synthetic and real waveform data to identify and eliminate possible problems and sources of error.

Synthetic Event Characterization

Using a synthetic waveform data set, the capabilities of the centroid moment tensor (CMT) inversion (Liu et al., 2004) were assessed. Figure 2 displays results from different parameterized inversions in an attempt to recover the solution in red at the top. Synthetics for the optimal solution and subsequent inversions were computed in model S2.9EA (Kustowski et al., 2008). Synthetics for the initial starting point were different in hypocenter and moment tensor elements to force the CMT inversion to recover the optimal solution. A simple CMT inversion, 6 parameters (black, top row), that does not solve for location or depth does a reasonable job in solution recovery. As more parameters are added, including depth, 7 parameters (black, middle row), and epicenter, 9 parameters (black, bottom row), the variance is further reduced as the original moment tensor and depth are well represented. The left and right columns of Figure 2 show inversions for only double couple (DC) or zero-trace (ZT) solutions. Zero-trace solutions perform better at representing the source as indicated by the smaller variance across the range of parameters used, 6–9. The new database of events will be built using the zero-trace (ZT) solutions.

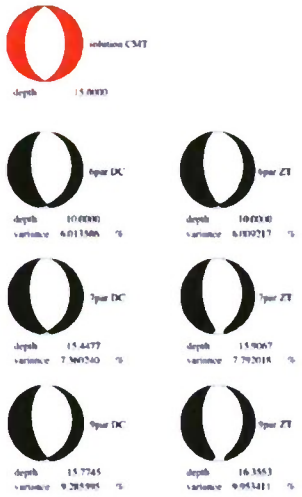

Figure 2. Performance of the CMT inversion to recover faulting parameters and source depth from a synthetic event (red) using several different parameterizations (black). Variance reductions and optimal depth for each parameterization are displayed beneath each moment tensor. See text for further explanation.

1D Event Characterization

Using the CMT inversion methodology of Liu et al. (2004), ~200 events in the Middle East were re-characterized using the 1D PREM model (Dziewonski and Anderson, 1981) at periods of 80 seconds and longer to accomplish two goals. First, the procedure of processing large amounts of data, comparing these to synthetics, and reevaluating

the source parameters and locations needed to be assessed and streamlined. This procedure needs to be straightforward and able to avoid problematic areas, as it will be used in the initial 3D event re-evaluation as well as two to three more times during the adjoint inversions. Second, problematic events and stations needed to be identified and removed before building the final waveform data set. Problematic stations and waveforms with dropouts and poorly characterized amplitude responses can negatively influence a CMT inversion. These stations were removed before any 3D CMT inversions were performed. Solutions from the long period 1D solutions are shown in Figure 3 (left). Faulting parameters and depths agree reasonably well with those from The Global CMT Project. Depths from the 1D model trend towards shallower depths, which is most likely due to the 3D model corrections used at The Global CMT Project.

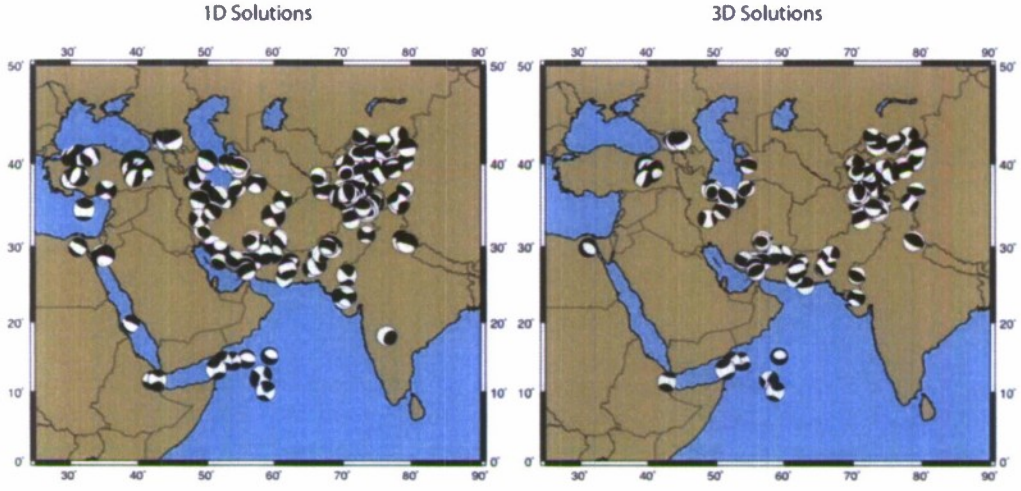

Figure 3. Comparison of new solutions using a 1D model, left, and 3D model, right. Fault plane solutions do not change appreciably when using either model, but the depths do change, especially when the events are deep. Catalog using the 1D model includes ~200 events, and the 3D model catalog currently has ~100 events (50% finished).

3D Event Characterization

The same events were also re-evaluated within the S2.9EA model (Kustowski et al., 2008) at a much shorter period of 25 seconds. Figure 3 (right) shows the current set of solutions, ~100 events (50% complete), inverted within the 3D wave speed model. Faulting solutions match well with the published solutions, and in contrast to the 1D solutions, the depths agree fairly well with published depths. While the solutions and depths match reasonably well when using either 1D or 3D wave speed models, the 3D wave speed synthetics use a much smaller minimum period, 25 seconds, that incorporates complicated body wave arrivals and more pronounced surface wave arrivals and dispersion.

Figure 4 displays vertical component data, black, and synthetics, red, for a single event on 2005/03/13 in the southern Zagros Mountains recorded by two stations to the north. Synthetics from the 1D PREM model at long and short periods are displayed in the first two columns. At long periods, the data and synthetics are relatively simple, with identifiable, small amplitude body wave arrivals and much larger amplitude, fundamental mode, surface wave arrivals. Synthetics match the absolute arrivals times rather well, but the amplitudes are misfit for each station at the longest period, 80 seconds. As shorter periods are included, middle column at 25 seconds, the synthetics remain simple arrivals as the data starts to shows dispersion due to traversing the continent, see 800 to 1100 seconds for station KURK.II.LHZ and 1000 to 1400 seconds for station KIEV.IU.LHZ. Body wave arrivals also show more complex propagation as compared to the 1D synthetics, including larger amplitudes, longer duration coda, 600 to 700 seconds for KURK.II.LHZ and 700 to 900 for KIEV.IU.LHZ in Figure 4 middle column. Simulations using the S2.9EA model (Kustowski et al., 2008) model reproduce the recorded data more closely than the 1D model at 25 seconds, Figure 4 right column. Use of the 3D wave speed model provides a more robust, shorter period estimation

of the faulting parameters without losing the essential, long period estimate of the moment/magnitude. The more complex propagation paths, represented by the waveform coda in the data and now the synthetics, do not influence the estimates of source epicenter, faulting parameters, and more importantly, source depth.

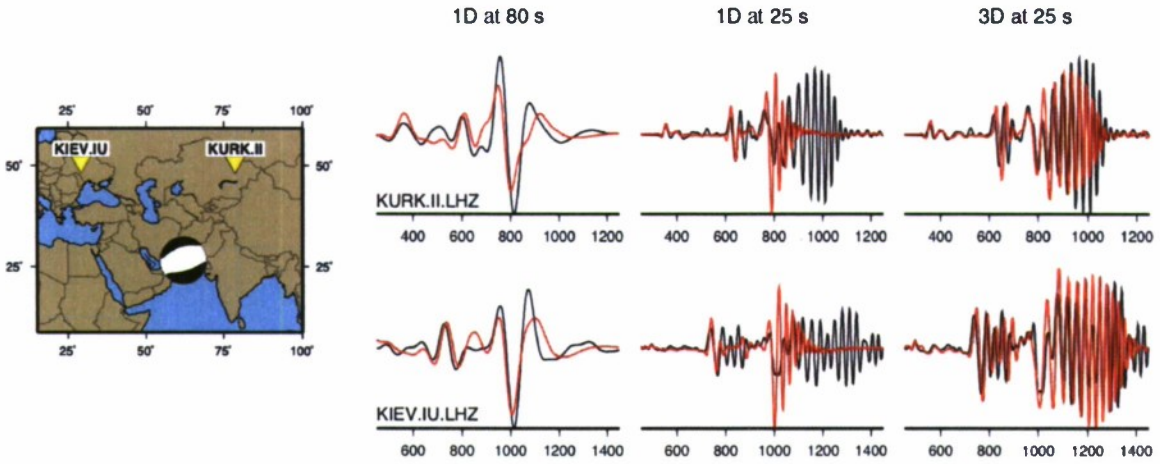

Figure 4. Comparison of vertical data and synthetics at long periods, 80 seconds, and short periods, 25 seconds, using 1D and 3D wave speed models. From the event shown in the map on the left, the data from two stations are compared to the different models. Inclusion of the 3D wave speed model improves the match between the data and synthetics, especially for the surface wave dispersion and the complex body wave arrivals.

Wave Speed Model Performance

As displayed in Figure 4, right column, the complexity of the waveforms is well represented by the 3D wave speed model, including the complex body wave arrivals and continental generated dispersion of the surface waves. While the general character of the wavefield is reproduced by the synthetics, the small variations in travel time and amplitude will be used to update the current iteration wave speed model within the adjoint tomography. Minor mismatches between data and synthetics are visible in a comparison for a single event on 2005/02/22 recorded at stations around the Middle East (Figure 5). Data from the tangential component, black, is compared with 3D synthetics, red, and plotted against azimuth to highlight different propagation paths. Paths towards the north show large amplitude, dispersive Love waves that are reasonably matched by the simulations, specifically the dispersion but not the amplitude. Recordings to the south show smaller, less dispersive Love waves as some paths include oceanic lithosphere and mantle (see waveforms at 180 degrees). Most of the surface wave energy is contained within the first pulse and the amplitude quickly diminishes with successive oscillations. Compared to the waveforms at 180 degrees, those at 350 degrees show an almost continuous surface wave amplitude of 300 to 400 seconds duration. These features are matched to first order by the current wave speed model, but improvements, primarily in amplitude, should be achievable through the adjoint, waveform methods.

Initial Adjoint Inversions

Using the mismatch between the observations and synthetic seismograms (e.g., Figure 5), an event kernel can be constructed using the adjoint method (Tromp et al., 2005) to guide updates of the current iteration, wave speed model. First, measurements between the data and synthetics are made automatically using the Flexwin tool (Maggi et al., 2009), which creates isolated data windows and generates metrics for each window, that are then used in the creation of the adjoint source. Windows, and thus the adjoint sources, are independent of any specific seismic phase and use only well matched data/synthetic pairs. Second, adjoint sources along with the full synthetic wavefield, are propagated in reverse time through the current iteration wave speed model. Third, the interactions

between the adjoint sources and the time-reversed wavefield, integrated over time, generate kernels specific to the measurement made, e.g., a simple difference between the data and synthetics.

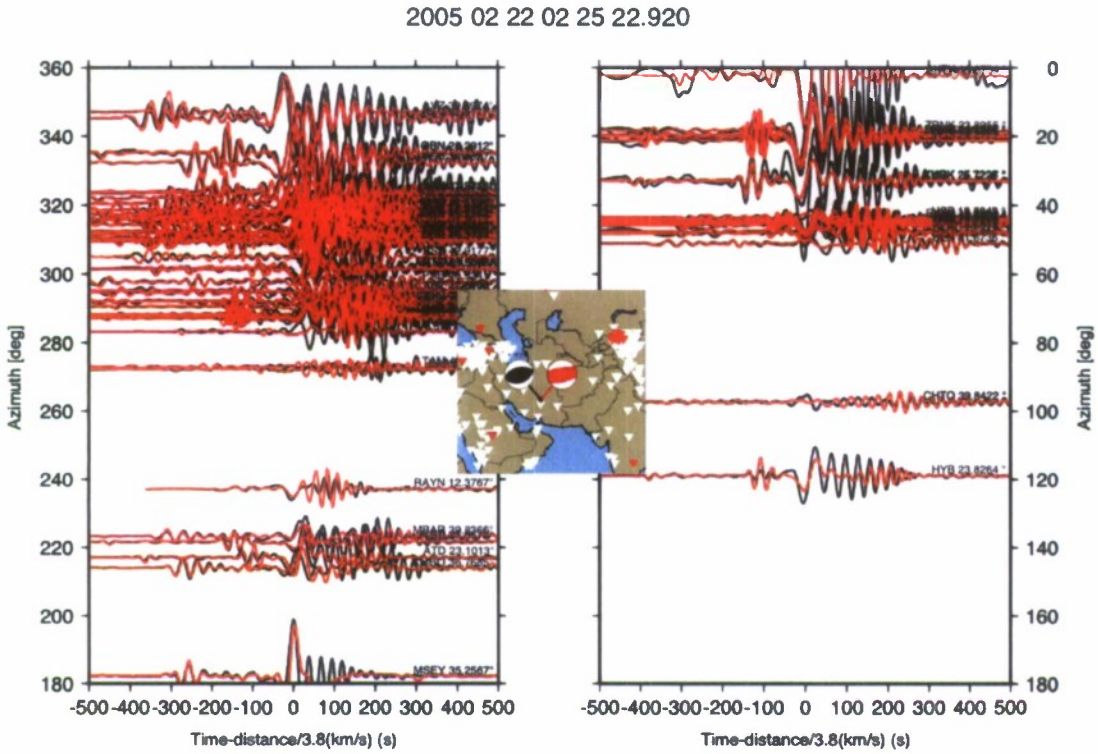

Figure 4. Comparison between tangential data and 3D synthetics for an event in the southern Zagros Mountains, map at center. Seismograms are plotted against azimuth to indicate the station coverage, wave field coherency, and to more readily identify where the wave speed model is deficient. Revised solution is in black and the globalcmt.org solution is in red.

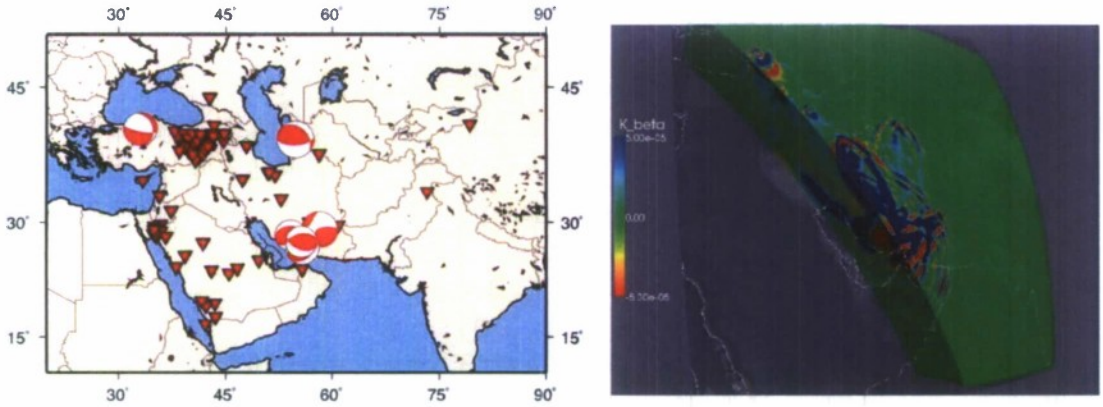

Figure 5. Example of a multiple-event kernel generated using the events and stations, left, for the Middle East. Colors for the shear kernel on the right indicate where the model requires adjustment. A north trending slice near the Persian Gulf demonstrates the kernel's volumetric nature.

Computation of a single-station, single-event kernel, or a multiple-station, single-event kernel, requires only one forward and one reverse simulation. Once all of the single-event kernels are created, multiple-event kernels for compressional modulus, shear modulus or density are produced by summing the individual event kernels together. Finally, it is these multiple-event kernels that are used to update the wave speed model. An example multiple-event kernel for a test set of 5 events is displayed in Figure 6. The map in Figure 6, left, shows the event and station locations used to construct the single-event kernels, and the multiple-event kernel for the shear modulus is shown on the right. A north trending slice through the multiple-event kernel near the Persian Gulf demonstrates the depth and volumetric nature of the kernel. Anticipated banana-doughnut shapes within the multiple-event kernel in Figure 6 are modified by a few important factors: 1) the simultaneous display of many source-to-station kernels, 2) kernels were computed in a 3D wave speed model generating more variable wave fields and many off great circle path arrivals, and 3) kernels presented here highlight regions where a mismatch is found between the forward and adjoint fields, i.e. where the model requires updating.

Initial tests, as displayed in Figure 6, demonstrate our ability to generate kernels from a set of events that are then required to update the current iteration wave speed model. Once all of the source re-evaluations are complete, the first in a series of model updates will commence. After a number of iterations, the sources will be reevaluated within the updated wave speed model to avoid mapping source errors into structural features. Iterations will continue until the misfit between the observations and synthetics has been sufficiently reduced.

CONCLUSIONS AND RECOMMENDATIONS

A seismic waveform database including source reinterpretations of the Middle East has been created. Work to characterize events within and around the Middle East has produced a large ~200 event database constrained by teleseismic and regional waveform CMT inversions. All inversion methods, the CMT inversion and previously used regional distance cut and paste (CAP) (Zhao and Helmberger, 1994) and teleseismic (Kikuchi and Kanamori, 1982) methods, provide robust estimates of source depth and faulting parameters. When used jointly, all offer an important verification of one another's result. Event characterization results from all inversions agree well with previously reported, routine determinations. Our initial tests using the 3D model S2.9EA have shown its ability to accurately simulate recorded seismic data within the Middle East at a minimum period of 25 seconds and a dramatic improvement over a simple 1D wave speed model at the same periods. Further, adjoint tomographic infrastructure for iteratively updating the current 3D wave speed model of the Middle East is in place and test inversions have already identified regions that will benefit from the adjoint methodology. We recommend, for the best possible 3D wave speed model result within the greater Middle East, that data from a wide range of sources be collected, quality checked, and added to this new waveform database, particularly seismic data from remote and/or sparsely instrumented areas.

REFERENCES

Dziewonski, A. M. and D. L. Anderson (1981). Preliminary reference Earth model, *Phys. Earth Planet Int.* 25: 297–356.

Kikuchi, M. and H. Kanamori (1982). Inversion of complex body waves, *Bull. Seism. Soc. Am.* 72: 491–506.

Komatitsch, D. and J. Tromp (1999). Introduction to the spectral-element method for 3-D seismic wave propagation, *Geophys. Jour. Int.* 139: 806–822.

Kustowski, B., G. Ekstrom, G., and A. M. Dziiwwonski (2008). The shear-wave velocity structure in the upper mantle beneath Eurasia, *Geophys. J. Int.* 174: 978–992.

Liu, Q., J. Polet, D. Komatitsch, and J. Tromp (2004). Spectral-Element Moment Tensor Inversions for Earthquakes in Southern California, *Bull. Seism. Soc. Am.* 94: 1748–1761.

Maggi, A., C. Tape, M. Chen, D. Chao, and J. Tromp (2009). An Automated time-window selection algorithm for seismic tomography, *Geophys. J. Int.* 178: 257–281.

Tromp, J., C. Tape, and Q. Liu (2005). Seismic tomography, adjoint methods, time reversal and banana-doughnut kernels, *Geophys. J. Int.* 160: 195–216.

Zhao, L. S. and D. V. Helmberger (1994). Source estimation from broadband regional seismograms, *Bull. Seism. Soc. Am.* 84: 91–104.